THE JOURNAL OF PHYSICAL CHEMISTRY B

Article

pubs.acs.org/JPCB

Physicochemical Characterization of Phosphopeptide/Titanium Dioxide Interactions Employing the Quartz Crystal Microbalance Technique

Anna I. K. Eriksson,[†] Katarina Edwards,[†,§] Anders Hagfeldt,[‡] and Víctor Agmo Hernández*,[†]

[†]Department of Chemistry−BMC, Uppsala University, Uppsala, Sweden

[‡]Department of Chemistry−Ångström, Uppsala University, Uppsala, Sweden

[§]FRIAS, School of Soft Matter Research, University of Freiburg, Freiburg, Germany

ABSTRACT: The rapidly growing field of phosphoproteomics has led to a strong demand for procedures enabling fast and reliable isolation and enrichment of phosphorylated proteins and peptides. During the past decade, several novel phosphopeptide enrichment methods based on the affinity of phosphoryl groups for titanium dioxide (TiO_2) have been developed and tested. The ultimate goal of obtaining comprehensive phosphoproteomes has, however, been found difficult to achieve and the obtained results often vary, dependent on the enrichment method and protocol used. In the present study, the physical chemistry of the phosphopeptide binding to TiO_2 is investigated by means of measurements using a quartz crystal microbalance with dissipation monitoring (QCM-D). Special emphasis is put on the effect of the degree of phosphorylation of the phosphopeptide, the impact of the primary amino acid structure, and the role of electrostatic interactions. The results show that, in general, adsorption of phosphopeptides follows the Langmuir model and that the affinity for the TiO_2 surface increases in a nonlinear fashion with increasing degree of phosphorylation. An exception was detected, however, where positive cooperativity between the peptides existed and the Langmuir model no longer applied. The source behind the cooperativity could be traced back to the primary amino acid structure and, more specifically, the presence of positively charged amino acids in positions that enable electrostatic interaction with phosphoryl groups on neighboring peptides. Regardless of the net peptide charge, the TiO_2−phosphopeptide interaction was for all phosphopeptides investigated found to be mainly of electrostatic origin. This study highlights and explains some of the most common problems with the TiO_2-based enrichment methods used today.

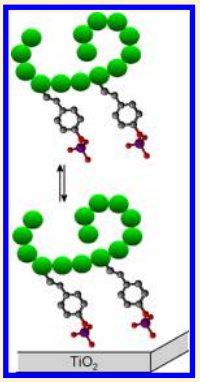

INTRODUCTION

One of the most common materials used in the hunt for new phosphoproteomes[1] and signaling pathways is titanium dioxide (TiO_2). Thus, TiO_2 is included in many of the methods for specific phosphopeptide enrichment used today,[2] e.g., metal oxide affinity chromatography (MOAC)[3−10] and direct on-target enrichment and separation.[11−16] However, an important problem encountered when these methods are used is the difficulty to obtain a comprehensive phosphoproteome. In most cases, the method favors the enrichment of either mono- or multiphosphorylated peptides. This leads to inconsistent results, as the resulting phosphoproteome for a certain protein differs considerably depending on the method used.[11,13,14] In order to help overcome these problems, an increased understanding of the mechanisms behind phosphopeptide−TiO_2 interaction and the factors affecting peptide adsorption are needed. Studies with molecules containing phosphonate[17−20] or phosphate[21,22] moieties have shown that these functionalizations confer high affinity for TiO_2 at acidic pH and that the most favorable bonding mode under these conditions is bidentate, which means that two oxygen atoms are involved in each bond (see Figure 1). However, no systematic studies have to date been made to analyze the physical chemistry of the binding of phosphorylated peptides to a TiO_2 surface.

Since peptides are quite complex molecules, there are several factors that may affect the phosphopeptide affinity for the titanium dioxide surface: e.g., the primary structure of the peptide, the position and number of phosphoryl groups, additional electrical charges on the peptide, etc. In this study, we used a quartz crystal microbalance with dissipation monitoring (QCM-D) to explore the impact of the degree of phosphorylation and the amino acid sequence on the phosphopeptide−TiO_2 interaction. Further, in order to more specifically examine the role of electrostatic interactions, we investigated the influence of buffer ionic strength on the peptide adsorption.

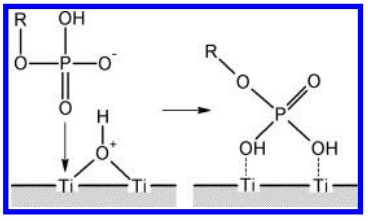

Figure 1. Schematic figure illustrating the adsorption of a phosphoryl group (−) on titanium dioxide (+) at acidic pH, which leads to a bidentate binding mode.

Received: October 15, 2012
Revised: December 17, 2012
Published: January 17, 2013

   dx.doi.org/10.1021/jp310161m | J. Phys. Chem. B 2013, 117, 2019−2025

EXPERIMENTAL SECTION

Materials and Chemicals. Custom-designed phosphopeptides were purchased from Thermo Scientific (Ulm, Germany). Commercially available peptides were purchased from Genscript (Piscataway, NJ). Trifluoroacetic acid (TFA >99%), sulfuric acid, hydrogen peroxide, sodium perchlorate, sodium dodecyl sulfate (SDS), acetonitrile (ACN), ammonium hydroxide solution (25−28%), phosphoric acid, sodium phosphate (mono- and dibasic), and sodium chloride were obtained from Sigma-Aldrich (Schnelldorf, Germany). All aqueous solutions were prepared in deionized water (18.4 MΩ cm) obtained from a Milli-Q system (Millipore, Bedford, MA). Titanium-coated QCM-D sensors were purchased from Q-Sense (Gothenburg, Sweden).

Peptides. Three custom-designed phosphopeptides with the same amino acid sequence and different (between 1 and 3) degrees of tyrosine phosphorylation (designated OnepY, TwopY, and ThreepY) were employed (Thermo Scientific). Three other commercially available peptides (Genscript) from commonly phosphorylated proteins were used to analyze eventual effects caused by the amino acid sequence. These peptides were derived from the Epidermal Growth Factor Receptor (EGFR, 1 × pY), Janus Kinase 2 (JAK, 2 × pY), and Insulin Receptor (IR, 3 × pY). To confirm specific phosphoryl−TiO_2 interaction, peptides with the same sequences but without phosphorylations were used as blanks (Genscript). All peptide solutions were prepared by dilution with 0.01% TFA (aq, pH 2.6) from a stock solution of 1 mg/mL in TFA buffer (ACN/water/TFA 50/49.9/0.1 (v/v)). The very acidic pH was chosen to avoid binding of carboxylic acid containing amino acids. The sequence, mass, and average charge of all peptides at the employed pH are shown in Table 1.

Table 1. Phosphopeptide Information, Including Amino Acid Sequence, Mass, and Average Charge at the Employed pH

name	sequence[a]	mass (Da)	av charge (pH = 2.6)
OnepY	ESYVESYVES-p**Y**-V	1533.60	−1
TwopY	ESYVES-p**Y**-VES-p**Y**-V	1613.60	−2
ThreepY	ES-p**Y**-VES-p**Y**-VES-p**Y**-V	1693.60	−3
EGFR	DADE-p**Y**-LIPQQG	1328.28	−1
JAK	VLPQD**K**E-p**Y**-p**Y**-**K**VKEPGE	2082.11	+1
IR	T**R**DI-p**Y**-ETD-p**Y**-p**Y**-**RK**	1862.68	0

[a]Phosphorylated tyrosine is marked with a -pY- and all charged amino acids are shown in bold.

QCM-D. The QCM-D technique, based on the inverse piezoelectric effect in quartz, allows monitoring both the mass adsorbed on the sensor surface and the dissipative properties of the adsorbed layer, and has been used to study the interactions, structure, and kinetics of many different biological systems (lipids, DNA, proteins, cells, etc.).[23−26] The two parameters that are monitored during the QCM-D measurement are the changes in oscillation frequency (f) and the dissipation factor (D). Adsorption of peptides on the sensor surface will be recorded as negative shifts in the frequency, since the extra mass load decreases the frequency of oscillation of the crystal. The dissipation, on the other hand, monitors the decay of oscillation of a crystal after the power is switched off, and gives an indication of the rigidity of the adsorbed film. For rigid films ($\Delta D \approx 0$), the measured change in frequency can be directly related to the mass adsorbed on the surface by using the Sauerbrey relationship

$$\Delta m = -CA\frac{\Delta f_n}{n} \quad (1)$$

where Δm is the adsorbed mass, C is the mass sensitivity constant (17.7 ng cm^{-2} Hz^{-1} at f_0 = 5 MHz), A is the active area of the sensor, and Δf_n is the frequency change at the nth overtone. The Sauerbrey relationship, however, only holds if the following assumptions are fulfilled: the adsorbed mass is small relative to mass of the quartz crystal, the molecules adsorbed form a rigid film, and the molecules are evenly distributed over the sensor area.[27,28]

All experiments were performed with an E1 QCM-D model and a pump connected downstream in the flow system. The temperature was set to 21 °C and the pump flow to 100 μL/min. Data was collected from the fundamental sensor frequency (5 MHz) as well as the 3rd, 5th, 7th, 9th, 11th, and 13th overtones. Mainly data from the third overtone was employed for quantitative determinations.

Pre-experimental Treatments. The titanium-coated QCM-D sensors were cleaned before each experiment. The cleaning procedure was different for new and used sensors. New QCM-D sensors were first cleaned thoroughly with 95% ethanol, dried with nitrogen gas, and then treated in hot piranha solution (3:1 sulfuric acid:hydrogen peroxide) for 20 s to oxidize the titanium surface. They were then rinsed with water and left in 99% ethanol for at least 5 min to wash away eventual rests of the chemicals. The sensors were dried with a gentle nitrogen flow before mounting into the instrument. Used QCM-D sensors were first put into 0.4 M NH_4OH (aq, pH 12) for at least 30 min to wash away the adsorbed phosphopeptides and then rinsed with MQ-water. The solution was then changed to 2% (w/w) SDS solution (aq) into which the sensors were incubated in for another 30 min before washed again with MQ-water and finally dried with nitrogen gas. When necessary, the piranha treatment was repeated. Results with new and reused sensors did not differ significantly.

Before the measurement, the QCM-D flow system (excluding the sensor) was incubated in PBS buffer (10 mM phosphate, 150 mM NaCl, pH 5.5) for 30 min to saturate all surfaces with PO_4^- and avoid phosphopeptide loss in the loop. After mounting of the sensor, a stable baseline from the solvent (0.01% TFA) was established before the measurement started.

Adsorption Experiments. Adsorption experiments were made with at least eight different peptide concentrations for all phosphopeptides, in order to create an adsorption isotherm plot for each. The measurements were made by loading the solution with the lowest peptide concentration and, once the recorded signal was stable, the system was rinsed with the original solvent until stability was reached again. This was repeated for the next lowest concentration, and so on until no significant frequency change upon increasing concentration was obtained. The frequency change due to phosphopeptide adsorption is the difference between the value of the baseline and the value after rinsing for each concentration.

Since the equilibrium is reached very slowly, the peptide solution was recirculated to avoid the use of large sample volumes. The recirculation started as soon as the loaded solution left the end of the out tube. The equilibrium concentration was then calculated by subtraction of the amount of adsorbed molecules from the total amount of molecules in the loading solution.

dx.doi.org/10.1021/jp310161m | J. Phys. Chem. B 2013, 117, 2019−2025

Repetitions of the measurements showed high reproducibility, discarding the possibility that peptides were lost in the loop. As verification for the specific phosphopeptide adsorption, the experiments were also repeated with the corresponding non-phopshorylated peptides in the same concentration range.

Kinetic Studies. Kinetic determinations were performed by directly loading the determined saturation concentration of each peptide on a clean sensor. The reason for the choice of a high concentration was to speed up the measurement time needed for equilibrium and to be able to simplify the analysis of the kinetics to pseudofirst order. The peptide solution was recirculated in the same way as before during the experiment.

Characterization of the Electrostatic Interactions. The role of electrostatic interactions was characterized with the three commercially available peptides with net charges ranging from +1 to −1. Adsorption experiments were performed as described above, but adding $NaClO_4$ (5, 25, or 50 mM) to the samples and the TFA buffer.

THEORY

Adsorption Models. The Langmuir adsorption model is the most simple and common model used to describe the adsorption behavior of molecules on a surface.[29] The Langmuir adsorption isotherm for the phosphopeptide−TiO_2 system becomes

$$\Gamma_{PT} = \frac{\Gamma_{PT,max} K_A [P]}{1 + K_A [P]} \quad (2)$$

where $[P]$ is the concentration of free phosphopeptides in the solution, K_A is the association equilibrium constant, Γ_{PT} is the surface concentration of adsorbed phosphopetides, and $\Gamma_{PT,max}$ is the maximum possible surface concentration of peptides. The Langmuir model is, however, only valid under certain assumptions, namely, all adsorption sites must be equal, each site can only hold one molecule, the molecules do not interact with each other, and the adsorption of one molecule does not affect the adsorption of another on the site next to it. Providing that these requirements are fulfilled, the parameters describing the adsorption can easily be calculated by means of several different methods based on linear regression. The Langmuir linear regression, proposed by Langmuir himself, is one of the most common.

$$\frac{[P]}{\Gamma_{PT}} = \frac{[P]}{\Gamma_{PT,max}} + \frac{1}{K_A \Gamma_{PT,max}} \quad (3)$$

Another linear regression method that can provide important information about the adsorption, also in cases when the Langmuir isotherm requirements are not fulfilled, is the Scatchard regression. This regression is given by

$$\frac{\Gamma_{PT}}{[P]} = K_A \Gamma_{PT,max} - K_A \Gamma_{PT} \quad (4)$$

The Scatchard plot ($\Gamma_{PT}/[P]$ versus Γ_{PT}) behavior, which has been thoroughly studied for several adsorption models, can not only show if the Langmuir model can be applied but also provide information about the applicability of alternative adsorption models, as the curvature of the plot gives useful indications about the adsorption mechanism.[30]

Kinetics. For the kinetic studies we used the Langmuir model, since during the first early stages of the experiment the degree of coverage is low and eventual peptide−peptide interactions causing cooperativity effects can be expected to be minimal due to the large separation between the adsorbed peptides. An expression for the rate of adsorption is created from the Langmuir model as follows

$$-\frac{d\Gamma_{PT}(t)}{dt} = k_a [P](t)\Gamma_T(t) - k_d \Gamma_{PT}(t) \quad (5)$$

where Γ_T is the surface concentration of binding sites on the TiO_2 surface. Under the used conditions (see Experimental Section), the peptide concentration can be considered constant, and thus the rate equation can be simplified assuming pseudo first order. This gives the boundary conditions that make it possible to solve eq 5.

$$[P](t) = [P_0] \quad (6a)$$

$$\Gamma_{PT}(t) + \Gamma_T(t) = \Gamma_{T,0} \quad (6b)$$

where $\Gamma_{T,0}$ is the total surface concentration of binding sites on the surface. The solution to eq 5 is

$$\Gamma_{PT}(t) = \frac{k_a [P_0] \Gamma_{T,0} (1 - e^{(-(k_a [P_0] + k_d)t)})}{k_a [P_0] + k_d} \quad (7)$$

The time constant $(1/(k_a[P_0] + k_d))$ can then be calculated by fitting the data to a simple exponential curve.

RESULTS

Adsorption Isotherms. The QCM-D results show that the dissipation/frequency ratio ($\Delta D/\Delta f$) was low for all peptides ($\ll$0.4), which indicates a rigid adsorbed structure. The Sauerbrey relationship (eq 1) was therefore used to calculate the adsorbed masses. An example of a measurement is shown in Figure 2. Measurements with the corresponding nonphosphorylated

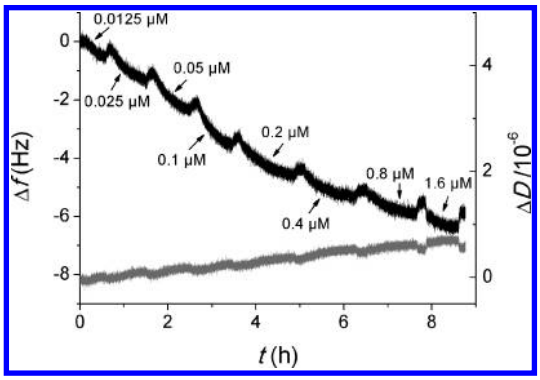

Figure 2. Example of a QCM-D measurement illustrating the binding of ThreepY to TiO_2. The shown frequency (black line) and dissipation factor (gray line) shifts represent the data obtained for the third overtone. The peptide bulk concentration is showed for each step.

peptides gave no significant frequency decrease, suggesting that the phosphoryl group is necessary for adsorption to occur. Phosphopeptide adsorption isotherms were created as plots of the fraction of surface coverage (θ, calculated by dividing the obtained Δf values by the frequency shift determined at maximum coverage, Δf_{max}) versus the equilibrium bulk concentration. The shapes of the obtained isotherms can be divided into two groups, hyperbolic or sigmodial, examples are shown in Figure 3a. Conversion of the isotherms to Scatchard plots, Figure 3b, shows that the sigmodial isotherm acquires the shape of a "sad mouth", i.e., concave down, while the hyperbolic isotherms become linear. The parameters describing the adsorption isotherms for all studied peptides are presented in Table 2.

dx.doi.org/10.1021/jp310161m | J. Phys. Chem. B 2013, 117, 2019−2025

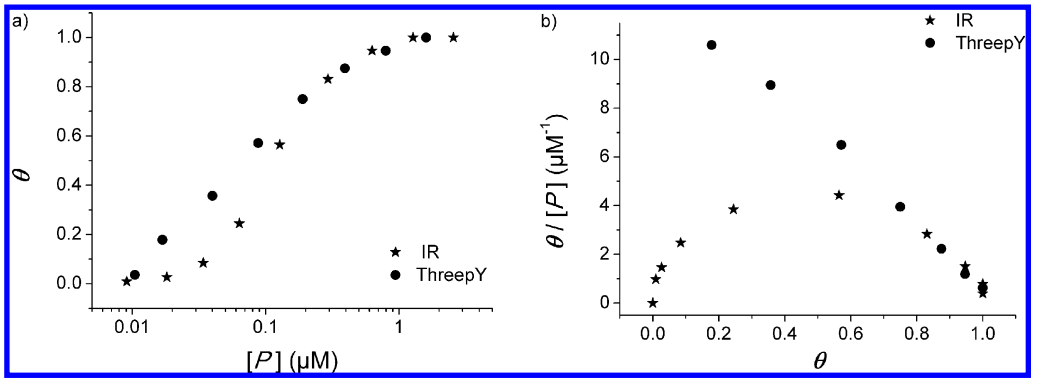

Figure 3. Representative examples of different phosphopeptide adsorption behaviors: (a) adsorption isotherms, and (b) Scatchard plots from the same data (recalculated according to eq 4).

Table 2. Summary of the Results Obtained from the QCM-D Adsorption Experiments for Each Phosphopeptide

peptide	isotherm shape	Scatchard shape	cooperativity	adsorption model	K_A[a] (μM^{-1})
OnepY	hyperbolic	linear	no	Langmuir	3.8 ± 0.56
TwopY	hyperbolic	linear	no	Langmuir	6.7 ± 0.51
ThreepY	hyperbolic	linear	no	Langmuir	13 ± 0.37
EGFR	hyperbolic	slightly concave up	not significant	Langmuir	3.2 ± 0.23
JAK	hyperbolic	slightly concave up	not significant	Langmuir	5.3 ± 0.55
IR	sigmodial	concave down	positive	2-layer BET	1.1 ± 0.47
					66 ± 27

[a]Values of the equilibrium association constants obtained from the used model. In the case of IR both the low concentration ($K_{A,S}$, first row) and the high concentration ($K_{A,L}$, second row) constants are shown.

The three custom-designed peptides have a hyperbolic isotherm shape and linear Scatchard plots and can therefore be described by the Langmuir model. The calculated equilibrium association constants are presented in Table 2 and show that the affinity for the titanium dioxide surface increases with the degree of phosphorylation.

Regarding the commercially available peptides, the EGFR and JAK isotherms are both hyperbolic and can after evaluation with Scatchard and Langmuir regressions be described by the Langmuir model. The calculated equilibrium association constants are of the same order of magnitude as observed for the custom peptides with the same degree of phosphorylation (Table 2). The IR isotherm, on the other hand, is sigmodial, and the Scatchard plot presents a maximum point, indicating positive cooperativity. Due to the inflection point in the IR isotherm, the data must be fitted with a polynomial model. The simplest polynomial model can be expressed from a modification of the Langmuir model, given by the ratio of two polynomials of the same order.[29]

$$\Gamma_{PT} = \Gamma_{PT,max}\frac{K_{A,1}[P] + 2K_{A,2}[P]^2 + ... + nK_{A,n}[P]^n}{1 + K_{A,1}[P] + K_{A,2}[P]^2 + ... + K_{A,n}[P]^n} \quad (8)$$

There are, however, several other possible polynomial models, all with different physical interpretations of the equilibrium constants. In order to find the right model for the IR isotherm, the experimental conditions must be considered. Since the surface used in this study can be assumed to remain homogeneous during the experiment and only one type of adsorption site exists for the phosphoryl group, the cooperativity has to occur due to interactions between the IR molecules. The chosen model must be able to differ between the IR−TiO_2 and the IR−IR interactions, and thus enable a comparison of the peptide−TiO_2 affinity for all six peptides. Gritti et al. have developed a liquid−solid extended BET isotherm for adsorption of molecules in solution on homogeneous surfaces. This model assumes that each molecule in the first adsorbed layer provides an adsorption site for the second layer and so on. Assuming formation of an infinite number of layers gives the following model equation[31]

$$\Gamma_{PT} = \Gamma_{PT,max}\frac{K_{A,S}[P]}{(1 - K_{A,L}[P])(1 - K_{A,L}[P] + K_{A,S}[P])} \quad (9)$$

where $K_{A,S}$ is the equilibrium association constant for the peptide−TiO_2 interaction occurring at low peptide bulk concentrations, while $K_{A,L}$ is the equilibrium association constant for the peptide−peptide interaction taking place at higher peptide concentrations. The equilibrium association constant for the peptide−TiO_2 interaction ($K_{A,S}$) should in principle correspond to the equilibrium association constant obtained from the Langmuir model in cases where no cooperative binding exists. Evaluation of the IR adsorption data showed, however, that the best fit was obtained if the model was changed to a finite number of two layers.[32]

$$\Gamma_{PT} = \Gamma_{PT,max}\frac{K_{A,S}[P] + 2K_{A,S}K_{A,L}[P]^2}{1 + K_{A,S}[P] + K_{A,S}K_{A,L}[P]^2} \quad (10)$$

The reason why the two-layer model fits better than the infinite model could be that the assumption of all adsorbed layers being equal is not fulfilled; i.e., the nature of the binding sites is not identical in each layer. Although it is possible that more layers are formed, the two-layer model provided an acceptable fitting without an excess of fitting parameters. The calculated values presented in Table 2 show that $K_{A,L}$ is much larger than $K_{A,S}$ and that the latter is closer in magnitude to the

dx.doi.org/10.1021/jp310161m | J. Phys. Chem. B 2013, 117, 2019−2025

K_A obtained for the custom-designed monophosphorylated peptide (OnepY) than to the K_A obtained for the triphosphorylated peptide (ThreepY). However, due to the very large relative error margins (~50% of the obtained value), the $K_{A,S}$ and $K_{A,L}$ values have to be used with care in further comparisons and calculations.

Kinetics. The first 30 min of the phosphopeptide binding reaction recorded in the kinetic experiments were fitted to a simple exponential curve. The obtained fitting parameters, together with the equilibrium dissociation constant ($K_D = 1/K_A$), were used to calculate the adsorption and desorption rate constants. The low concentration association constant, $K_{A,S}$, was used for the IR peptide. The calculated rate constants are shown in Table 3.

Table 3. Summary of the Results Obtained from the QCM-D Kinetic Experiments for Each Phosphopeptide

peptide	K_D[a] (μM)	k_a[b]/10^{-3} (s^{-1} μM^{-1})	k_d[b]/10^{-4} (s^{-1})
OnepY	0.26 ± 0.04	5.0 ± 0.24	13 ± 1.89
TwopY	0.15 ± 0.01	4.3 ± 0.05	6.4 ± 0.47
ThreepY	0.08 ± 0.00	5.7 ± 0.05	4.5 ± 0.13
EGFR	0.31 ± 0.02	1.3 ± 0.02	4.0 ± 0.30
JAK	0.19 ± 0.02	2.6 ± 0.05	5.0 ± 0.51
IR	0.88 ± 0.36	1.4 ± 0.30	12 ± 2.35

[a]Obtained from the equilibrium association constants ($K_{A,S}$ for IR). [b]Calculated from the pseudo-first-order rate equation (eq 7).

Electrostatic Interactions. The addition of $NaClO_4$ to the system clearly had an effect on the adsorption of all three commercially available peptides. Regardless of the peptide net charge, the isotherms were upon addition of salt shifted toward higher peptide concentrations. Isotherms recorded for IR at $NaClO_4$ concentrations between 0 and 50 mM are displayed in Figure 4. Equilibrium association constants obtained at 25 mM $NaClO_4$ for EGFR, JAK, and IR, respectively, are shown in Table 4.

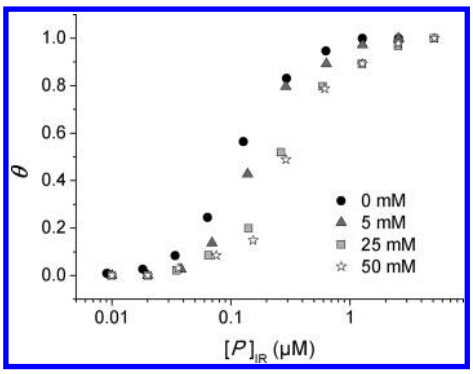

Figure 4. Adsorption isotherms of IR obtained at different concentrations of $NaClO_4$ in the bulk solution.

DISCUSSION

Degree of Phosphorylation. The analysis of the adsorption isotherms obtained for the three custom-designed peptides (OnepY, TwopY, and ThreepY), differing only in degree of phosphorylation, shows that the phosphopeptide adsorption on TiO_2 in general follows the Langmuir model. In light of the fact that the phosphoryl units constitute the only charged groups in these custom-designed peptides, and that the peptides were specifically designed to be water-soluble, i.e., they have no large hydrophobic parts, this finding comes as no surprise. Importantly, also the EGFR and the net positively charged JAK peptide display adsorption behavior in agreement with the Langmuir model. However, as revealed by the data collected for the IR peptide, the adsorption can be complicated by peptide−peptide interactions leading to cooperative behavior. The origin of the cooperative binding and its correlation to the peptide amino acid sequence will be discussed in later sections of this report.

Table 4. Summary of the Results Obtained from the QCM-D Electrostatic Experiments for Each Commercial Available Phosphopeptide

peptide	$K_{A,0}$ (μM^{-1})	$K_{A,2S}$ (μM^{-1})
EGFR	3.2 ± 0.23	2.1 ± 0.18
JAK	5.3 ± 0.55	2.3 ± 0.52
IR[a]	1.1 ± 0.47	0.9 ± 0.40
	66 ± 27	14 ± 7.3

[a]Show both the low concentration ($K_{A,S}$, 1st row) and the high concentration ($K_{A,L}$, 2nd row) constants.

The thermodynamic results presented in Table 2 clearly show that the affinity of the phosphopeptides for the TiO_2 surface increases significantly with the degree of phosphorylation. Interestingly, the values in Table 2 show that the equilibrium association constants increase ~2-fold for each extra phosphorylation site, i.e., $K_{A,TwopY} \approx 2 \times K_{A,OnepY}$ and $K_{A,ThreepY} \approx 2 \times K_{A,TwopY}$. This indicates a power of 2, rather than a linear, relationship between the degree of phosphorylation and the equilibrium association constant. Moreover, it is noteworthy that the two commercially available peptides, EGFR and JAK, that followed the Langmuir model display association constants in the same range as the corresponding custom peptide with the same degree of phosphorylation.

The kinetic results obtained for the custom peptides (see Table 3) reveal that the dissociation rate constant decreases significantly with increasing degree of phosphorylation, while the association rate constant does not follow any clear trend. This indicates that the trend in affinity is set by the desorption rate. It is also shown that the adsorption process is relatively slow regardless of the degree of phosphorylation or the presence of cooperativity. This implies that, on a large enough surface, quantitative adsorption from a given sample may require between several minutes and a few hours (depending on the peptide concentration and available surface area). Furthermore, the fact that multiphosphorylated peptides bind more irreversibly to the substrate may account for the bias of TiO_2-based MOAC enrichment toward monophosphorylated peptides. In MOAC, a significant proportion of the multiphosphorylated fraction may remain bound to the substrate, accounting for their poor detection. Noteworthy, this bias toward monophosphorylated peptides is not observed in on-target enrichment and separation approaches,[16] which allow detection of more or less irreversibly bound peptides.

Amino Acid Sequence. Two of the commercially available peptides, EGFR and JAK, display, similar to the custom-designed peptides, adsorption behavior compatible with the Langmuir model. The third peptide, IR, shows a very different adsorption behavior, as can be seen in Table 2 and Figure 3. As mentioned above, the data suggest that the peptide molecules bind in a cooperative manner; i.e., once one molecule adsorbs, the adsorption of the next one is facilitated. The observed cooperative behavior most likely stems from attractive peptide−peptide

dx.doi.org/10.1021/jp310161m | J. Phys. Chem. B 2013, 117, 2019−2025

interactions, but a matter open for discussion is what particular features of the amino acid sequence make the IR peptide prone to such interactions. The two main possible ways of interaction are either hydrophobic or electrostatic interactions. Hydrophobic interactions between IR peptides are unlikely to cause the observed cooperativity, since IR is the most hydrophilic peptide in this study, containing only one hydrophobic amino acid (I) in the whole sequence. On the other hand, the IR amino acid sequence (Table 1) shows that the three positively charged amino acids are located at the ends of this peptide. It could be speculated that one, or possibly both, of these positive ends are capable of engaging in electrostatic interactions with a phosphoryl group on another IR peptide. The fact that the relative position of positively charged amino acids can have a strong effect on the adsorption behavior (compare, e.g., isotherms recorded for JAK and IR) is an interesting and potentially important finding, especially since one of the most common digestion enzymes, trypsin, cleaves after R and K, i.e., amino acids that are positively charged at the conditions commonly employed for phosphopeptide enrichment. Our findings suggest that peptides obtained after tryptic digestion are likely to display a binding behavior similar to that of IR; i.e, they are likely to show cooperativity. This conclusion needs, however, to be verified in future investigations.

The surprisingly low $K_{A,S}$ value found for the triphosphorylated peptide IR suggests, moreover, that the amino acid sequence can affect also the peptide−TiO_2 affinity. As electrostatic interactions were found to be important for the affinity (see next section), it might be suggested that the two positively charged amino acids positioned next to two of the phosphorylated tyrosines (Table 1) decrease the IR−TiO_2 affinity.

Electrostatic Interaction. The results presented in Table 4 and Figure 4 show that electrostatic interactions play an important role in controlling the affinity of the phosphoryl group of phosphopeptides for TiO_2. In the presence of 25 mM $NaClO_4$ no significant difference in affinity can be observed for EGFR and JAK, indicating that the electrostatic contribution to the TiO_2−phosphoryl interaction is screened. The isotherm for the triphosphorylated peptide (IR) is in a similar manner shifted toward higher peptide concentrations (Figure 4). This indicates that the initial adsorption of IR peptides to the surface is screened by the present ions. However, the extent of this screening cannot be determined accurately given the large errors obtained for the association constants of the IR−TiO_2 interaction. A similar situation is observed in the case of the peptide−peptide interaction. Addition of salt decreases $K_{A,L}$ but the absolute difference between the association constant values obtained in the presence and absence of salt is within the range of the determined error margins, and, unfortunately, the effect of the present electrolyte cannot be conclusively established.

CONCLUSIONS

This study shows the possibility to use the QCM-D technique for investigations of the physical chemistry behind the phosphopeptide enrichment process on TiO_2. The reported results from the adsorption experiments demonstrate several important features. First, regardless of the overall peptide net charge, the phosphopeptide adsorption is heavily influenced by electrostatic interactions between the phosphoryl group in the peptide and the positively charged TiO_2 surface. Second, if there is no peptide−peptide interaction, the general phosphopeptide adsorption follows the Langmuir model. Third, the affinity for the TiO_2 surface increases with increasing degree of phosphorylation, but may be reduced by the presence of interfering charges on the peptide or by electrostatic screening from bulk ions.

The fact that the peptide primary structures can affect the surface affinity (as has been reported also by Lucrèce et al[33]), as well as induce cooperative binding behavior, makes it difficult to create a general rule for how the adsorption correlates to the number of peptide phosphorylation sites. Further, depending on the separation or enrichment protocol used, the binding behavior may vary, and the obtained results can therefore differ for the same peptide composition. In addition, so far only tyrosine phosphorylated peptides have been studied, representing the starting point for a broader characterization of all factors and parameters that may affect the phosphopeptide−TiO_2 interaction. Further investigations should aim to explore eventual affinity differences depending on the phosphorylated amino acid (tyrosine, threonine, or serine).

The observations and insights gained from the current study are helpful to understand the mechanisms leading to phosphopeptide enrichment in TiO_2-based methods. Furthermore, the QCM-D method employed has been revealed as a useful tool to study different aspects of the peptide−TiO_2 interaction. This opens a wide window for future research as, e.g., the characterization of the effect on the phosphopeptide−TiO_2 affinity of additives such as 2,5-dihydroxybenzoic acid and other organic acids, which are commonly used to increase the selectivity of phosphopeptide enrichment procedures.

Our results, moreover, expose the difficulties involved in creating a single, straightforward method capable of providing comprehensive phosphoproteomes. A successful enrichment method should most likely include several enrichment/elution steps performed under different conditions (salt concentrations, pH values), or be based on a protocol where these conditions are gradually changed during the procedure. For instance, the use of eluants with different pH values to improve phosphopeptide mapping has been successfully applied previously.[34] Another possibility is that salt concentration gradients could lead to the separation of the phosphopeptides according to their degree of phosphorylation. By employing these approaches, the commonly observed bias toward either mono- or multiphosphorylated peptides could hopefully be overcome.

AUTHOR INFORMATION

Corresponding Author

*Phone: +46 (0) 18 471 3635. Fax: +46 (0) 18 471 3654. E-mail: victor.agmo@kemi.uu.se.

Notes

The authors declare no competing financial interest.

ACKNOWLEDGMENTS

Financial support from the Swedish Research Council is acknowledged.

REFERENCES

(1) Tichy, A.; Salovska, B.; Rehulka, P.; Klimentova, J.; Vavrova, J.; Stulik, J.; Hernychova, L. Phosphoproteomics: Searching for a Needle in a Haystack. *J. Proteomics* **2011**, *74*, 2786−2797.

(2) Dunn, J. D.; Reid, G. E.; Bruening, M. L. Techniques for Phosphopeptide Enrichment Prior to Analysis by Mass Spectrometry. *Mass Spectrom. Rev.* **2010**, *29*, 29−54.

(3) Larsen, M. R.; Thingholm, T. E.; Jensen, O. N.; Roepstorff, P.; Jorgensen, T. J. D. Highly Selective Enrichment of Phosphorylated Peptides from Peptide Mixtures Using Titanium Dioxide Microcolumns. *Mol. Cell. Proteomics* **2005**, *4*, 873−886.

(4) Pinkse, M. W. H.; Uitto, P. M.; Hilhorst, M. J.; Ooms, B.; Heck, A. J. R. Selective Isolation at the Femtomole Level of Phosphopeptides from Proteolytic Digests Using 2D-Nanolc-ESI-MS/MS and Titanium Oxide Precolumns. *Anal. Chem.* **2004**, *76*, 3935−3943.
(5) Kweon, H. K.; Hakansson, K. Selective Zirconium Dioxide-Based Enrichment of Phosphorylated Peptides for Mass Spectrometric Analysis. *Anal. Chem.* **2006**, *78*, 1743−1749.
(6) Klemm, C.; Otto, S.; Wolf, C.; Haseloff, R. F.; Beyermann, M.; Krause, E. Evaluation of the Titanium Dioxide Approach for MS Analysis of Phosphopeptides. *J. Mass Spectrom.* **2006**, *41*, 1623−1632.
(7) Han, G. H.; Ye, M. L.; Zou, H. F. Development of Phosphopeptide Enrichment Techniques for Phosphoproteome Analysis. *Analyst* **2008**, *133*, 1128−1138.
(8) Thingholm, T. E.; Jorgensen, T. J. D.; Jensen, O. N.; Larsen, M. R. Highly Selective Enrichment of Phosphorylated Peptides Using Titanium Dioxide. *Nat. Protoc.* **2006**, *1*, 1929−1935.
(9) Thingholm, T. E.; Larsen, M. R.; Ingrell, C. R.; Kassem, M.; Jensen, O. N. TiO_2-Based Phosphoproteomic Analysis of the Plasma Membrane and the Effects of Phosphatase Inhibitor Treatment. *J. Proteome Res.* **2008**, *7*, 3304−3313.
(10) Chen, C. T.; Chen, Y. C. Fe_3O_4/TiO_2 Core/Shell Nanoparticles as Affinity Probes for the Analysis of Phosphopeptides Using TiO_2 Surface-Assisted Laser Desorption/Ionization Mass Spectrometry. *Anal. Chem.* **2005**, *77*, 5912−5919.
(11) Qiao, L.; Roussel, C.; Wan, J. J.; Yang, P. Y.; Girault, H. H.; Liu, B. H. Specific On-Plate Enrichment of Phosphorylated Peptides for Direct MALDI-TOF MS Analysis. *J. Proteome Res.* **2007**, *6*, 4763−4769.
(12) Torta, F.; Fusi, M.; Casari, C. S.; Bottani, C. E.; Bachi, A. Titanium Dioxide Coated MALDI Plate for on Target Analysis of Phosphopeptides. *J. Proteome Res.* **2009**, *8*, 1932−1942.
(13) Niklew, M. L.; Hochkirch, U.; Melikyan, A.; Moritz, T.; Kurzawski, S.; Schluter, H.; Ebner, I.; Linscheid, M. W. Phosphopeptide Screening Using Nanocrystalline Titanium Dioxide Films as Affinity Matrix-Assisted Laser Desorption Ionization Targets in Mass Spectrometry. *Anal. Chem.* **2010**, *82*, 1047−1053.
(14) Eriksson, A.; Bergquist, J.; Edwards, K.; Hagfeldt, A.; Malmstrom, D.; Hernandez, V. A. Optimized Protocol for On-Target Phosphopeptide Enrichment Prior to Matrix-Assisted Laser Desorption-Ionization Mass Spectrometry Using Mesoporous Titanium Dioxide. *Anal. Chem.* **2010**, *82*, 4577−4583.
(15) Wang, H.; Duan, J. C.; Cheng, Q. Photocatalytically Patterned TiO(2) Arrays for On-Plate Selective Enrichment of Phosphopeptides and Direct MALDI MS Analysis. *Anal. Chem.* **2011**, *83*, 1624−1631.
(16) Eriksson, A.; Bergquist, J.; Edwards, K.; Hagfeldt, A.; Malmstrom, D.; Hernandez, V. A. Mesoporous TiO(2)-Based Experimental Layout for On-Target Enrichment and Separation of Multi- and Monophosphorylated Peptides Prior to Analysis with Matrix-Assisted Laser Desorption-Ionization Mass Spectrometry. *Anal. Chem.* **2011**, *83*, 761−766.
(17) Guerrero, G.; Mutin, P. H.; Vioux, A. Anchoring of Phosphonate and Phosphinate Coupling Molecules on Titania Particles. *Chem. Mater.* **2001**, *13*, 4367−4373.
(18) Pawsey, S.; McCormick, M.; De Paul, S.; Graf, R.; Lee, Y. S.; Reven, L.; Spiess, H. W. H-1 Fast MAS NMR Studies of Hydrogen-Bonding Interactions in Self-Assembled Monolayers. *J. Am. Chem. Soc.* **2003**, *125*, 4174−4184.
(19) Luschtinetz, R.; Frenzel, J.; Milek, T.; Seifert, G. Adsorption of Phosphonic Acid at the TiO(2) Anatase (101) and Rutile (110) Surfaces. *J. Phys. Chem. C* **2009**, *113*, 5730−5740.
(20) Di Valentin, C.; Costa, D. Anatase TiO_2 Surface Functionalization by Alkylphosphonic Acid: A DFT+D Study. *J. Phys. Chem. C* **2012**, *116*, 2819−2828.
(21) Connor, P. A.; McQuillan, A. J. Phosphate Adsorption onto TiO_2 from Aqueous Solutions: An In Situ Internal Reflection Infrared Spectroscopic Study. *Langmuir* **1999**, *15*, 2916−2921.
(22) Engholm-Keller, K.; Larsen, M. R. Titanium Dioxide as Chemo-Affinity Chromatographic Sorbent of Biomolecular Compounds - Applications in Acidic Modification-Specific Proteomics. *J. Proteomics* **2011**, *75*, 317−328.
(23) Rodahl, M.; Hook, F.; Fredriksson, C.; Keller, C. A.; Krozer, A.; Brzezinski, P.; Voinova, M.; Kasemo, B. Simultaneous Frequency and Dissipation Factor QCM Measurements of Biomolecular Adsorption and Cell Adhesion. *Faraday Discuss.* **1997**, *107*, 229−246.
(24) Fredriksson, C.; Kihlman, S.; Rodahl, M.; Kasemo, B. The Piezoelectric Quartz Crystal Mass and Dissipation Sensor: A Means of Studying Cell Adhesion. *Langmuir* **1998**, *14*, 248−251.
(25) Cho, N.-J.; Frank, C. W.; Kasemo, B.; Hook, F. Quartz Crystal Microbalance with Dissipation Monitoring of Supported Lipid Bilayers on Various Substrates. *Nat. Protoc.* **2010**, *5*, 1096−1106.
(26) Becker, B.; Cooper, M. A. A Survey of the 2006−2009 Quartz Crystal Microbalance Biosensor Literature. *J. Mol. Recognit.* **2011**, *24*, 754−787.
(27) Dixon, M. C. Quartz Crystal Microbalance with Dissipation Monitoring: Enabling Real-Time Characterization of Biological Materials and Their Interactions. *J. Biomol. Tech.* **2008**, *19*, 151−158.
(28) Reviakine, I.; Johannsmann, D.; Richter, R. P. Hearing What You Cannot See and Visualizing What You Hear: Interpreting Quartz Crystal Microbalance Data from Solvated Interfaces. *Anal. Chem.* **2011**, *83*, 8838−8848.
(29) Guiochon, G.; Felinger, A.; Shirazi, D. G.; Katti, A. M. *Fundamentals of Preparative and Nonlinear Chromatography*, 2nd ed.; Elsevier: Amsterdam, 2006.
(30) Samuelsson, J.; Arnell, R.; Fornstedt, T. Potential of Adsorption Isotherm Measurements for Closer Elucidating of Binding in Chiral Liquid Chromatographic Phase Systems. *J. Sep. Sci.* **2009**, *32*, 1491−1506.
(31) Gritti, F.; Piatkowski, W.; Guiochon, G. Comparison of the Adsorption Equilibrium of a Few Low-Molecular Mass Compounds on a Monolithic and a Packed Column in Reversed-Phase Liquid Chromatography. *J. Chromatogr. A* **2002**, *978*, 81−107.
(32) Gritti, F.; Guiochon, G. Influence of a Buffered Solution on the Adsorption Isotherm and Overloaded Band Profiles of an Ionizable Compound. *J. Chromatogr. A* **2004**, *1028*, 197−210.
(33) Lucrece, M.; Emmanuelle, S.; Fabienne, B.; Sandrine, S.; Olivier, L.; Gerard, B. Sequence-Dependent Enrichment of a Model Phosphopeptide: A Combined MALDI-TOF and NMR Study. *Anal. Chem.* **2011**, *83*, 3003−3010.
(34) Park, S.-S.; Maudsley, S. Discontinuous pH Gradient-Mediated Separation of TiO_2-Enriched Phosphopeptides. *Anal. Biochem.* **2011**, *409*, 81−88.